JOURNAL OF BACTERIOLOGY, June 1995, p. 3370–3378 Vol. 177, No. 12
0021-9193/95/$04.00+0
Copyright © 1995, American Society for Microbiology

The Proline-Rich P65 Protein of *Mycoplasma pneumoniae* Is a Component of the Triton X-100-Insoluble Fraction and Exhibits Size Polymorphism in the Strains M129 and FH

THOMAS PROFT, HELMUT HILBERT, GERLINDE LAYH-SCHMITT, AND RICHARD HERRMANN*

Zentrum für Molekulare Biologie Heidelberg, Mikrobiologie, Universität Heidelberg, 69120 Heidelberg, Germany

Received 31 October 1994/Accepted 8 April 1995

Previously, we described the identification of a novel *Mycoplasma pneumoniae* M129 protein, named P65 because of its apparent molecular mass of 65 kDa estimated by sodium dodecyl sulfate-polyacrylamide gel electrophoresis (T. Proft and R. Herrmann, Mol. Microbiol. 13:337–348, 1994). DNA sequence analysis of the P65 open reading frame (*orfp*65), however, revealed an ORF encoding a protein with a molecular weight of 47,034. This discrepancy can be explained by the unusual amino acid composition of this protein. According to the deduced amino acid sequence, the N-terminal half of P65 contains several penta- and hexapeptides (DPNAY and DPNQAY) forming a proline-rich acidic domain. Secondary-structure predictions indicated β-sheets and turns within that region, suggesting an extended and rigid conformation. Near the C terminus of P65 the tripeptide Arg-Gly-Asp (RGD) was found. This motif is known to play an important role in binding of extracellular matrix proteins to integrins. P65 could be located exclusively to the Triton X-100-insoluble cell fraction. The results of immunofluorescence microscopy and of immunoadsorption experiments indicated that P65 carries surface-exposed regions. Mild treatment of whole cells with proteases resulted in cleavage of a limited amount of P65 molecules, suggesting either that only a small percentage of P65 molecules are exposed on the surface or that protease cleavage is hampered by a compact protein conformation or by binding of an unknown component to P65. P65 exhibits size polymorphism in *M. pneumoniae* M129 and FH. This is caused by an intragenetic duplication of a 54-bp sequence within the FH *orfp*65. As a consequence, the number of DPNAY pentapeptides increased from 9 to 12 repeats in the FH strain.

Mycoplasma pneumoniae is an extracellular pathogen of the human respiratory tract (26, 46) causing histopathological changes of lung epithelial cells, usually in older children and young adults (18). A critical step in bacterial colonization of the host cells is the specific adhesion to host cell receptors, mediated by bacterial adhesins. In *M. pneumoniae*, the P1 adhesin (3, 17, 25, 26) and the adhesin-related 30-kDa protein (4, 10) have been identified. Both proteins are located mainly in a tip structure that functions as the attachment organelle of the bacterium. It could be demonstrated, by nearest-neighbor analysis with a hydrophilic chemical cross-linker, that the product of open reading frame 6 (ORF6) of the P1 operon (28), a 40-kDa protein and 90-kDa protein (9, 34, 50) are located in close proximity to the P1 adhesin on the cell surface (35).

Scanning and transmission electron microscope analyses of *M. pneumoniae* cells grown on grids and pretreated with Triton X-100 revealed a rodlike tip structure and a network of filamentous strands (22, 41). Krause and coworkers identified a set of high-molecular-weight proteins (HMW1 to HMW5) which play an important role in cytadherence (30, 31, 51–53) and appear to be involved in formation of a cytoskeletonlike structure (38). These proteins, but also a certain percentage of the P1 adhesin, partition in the detergent-insoluble fraction (Triton shell) after Triton X-100 extraction (29, 52, 53). Cytadherence-negative variants that lack the HMW proteins show a rather random distribution of P1 on the cell surface, and the bacteria are no longer virulent (31). Ogle et al. (44) reported the first sequence analysis of a complete gene encoding a cytadherence-associated protein (HMW3). The deduced amino acid sequence revealed an acidic protein with an unusually high proline content of 13.5%. Secondary-structure predictions suggested the probability for a rigid and extended protein conformation.

Evidence for a bacterial cytoskeleton has also been reported for the wall-less archaebacterium *Thermoplasma acidophilum* (24). In general, a bacterial interconnecting protein network seems to be important for preserving the integrity of wall-less cells and for asymmetric distribution of membrane proteins. So far, significant sequence homologies between eucaryotic cytoskeletal proteins and any bacterial protein have not been found. Recently we reported the identification and characterization of the *M. pneumoniae* protein P65 localized exclusively in the Triton X-100-insoluble fraction (45).

Since proteins from this cell fraction are, in analogy to eucaryotic cells, promising candidates for cytoskeleton-forming or cytoskeleton-associated proteins, we describe the further biochemical characterization of P65 and DNA analysis of the corresponding gene. Moreover, we show a size polymorphism in P65 and its genetic basis in two *M. pneumoniae* strains, M129 and FH.

* Corresponding author. Mailing address: Zentrum für Molekulare Biologie Heidelberg, Mikrobiologie, Universität Heidelberg, Im Neuenheimer Feld 282, 69120 Heidelberg, Germany. Phone: 49-6221-56 6827. Fax: 49-6221-56 5893.

MATERIALS AND METHODS

Organisms and growth conditions. *M. pneumoniae* M129 (broth passage 21) (ATCC 29342) and *M. pneumoniae* FH (2) cultures were grown at 37°C in Roux flasks (137 cm^2) containing 100 ml of modified Hayflick medium (23) supplemented with 20% horse serum. After 48 h, glass-attached cells were washed three times with phosphate-buffered saline (PBS; 0.15 M NaCl, 10 mM sodium phosphate, pH 7.4), scraped off, and resuspended in PBS. The cells were pelleted at 6,000 × *g* for 10 min at 4°C and stored at −70°C.

Escherichia coli XL1-Blue cells (7) were grown in Luria-Bertani broth at 37°C.

Fractionation of the Triton X-100-insoluble fraction. The Triton X-100 extraction was performed as previously described (45). *M. pneumoniae* cells were suspended in 10 mM Tris-HCl (pH 7.5)–150 mM NaCl–10 U of aprotinin per ml (Boehringer, Mannheim, Germany) to a concentration of 2 mg of protein per ml and extracted with 2% (vol/vol) Triton X-100 (Sigma). The Triton X-100-insoluble material derived from 1 ml of cell suspension was collected by centrifugation (14,000 × *g* for 30 min). The pellet was resuspended in 1 ml of 0.6 M KCl–1 mM EDTA–10 U of aprotinin per ml and incubated for 30 min at room temperature. Thereafter, the insoluble material was again collected by centrifugation and incubated for 30 min in 1 M $MgCl_2$ at room temperature. The procedure was repeated step by step with increasing concentrations of $MgCl_2$ (2, 3, and 4 M). By the same protocol, the extraction was also carried out with 1, 2, 3, and 4 M potassium iodine (KJ) and with 2, 4, 6, and 8 M urea. The solubilized proteins were precipitated by adding 0.15 volume of 3 M trichloracetic acid to the various supernatants. All samples were suspended in 300 μl of sample buffer for immunoblot analysis or silver-stained sodium dodecyl sulfate-polyacrylamide gel electrophoresis (SDS-PAGE).

SDS-PAGE and Western blotting (immunoblotting). *M. pneumoniae* proteins were subjected to SDS-PAGE as described by Laemmli (33). The separated proteins were electrophoretically transferred to nitrocellulose sheets (Schleicher & Schuell) with 5 mA/cm^2 by using a semidry blot apparatus (Biometra) with transfer buffer (25 mM Tris, 150 mM glycine, 10% methanol, pH 8.3). The sheets were blocked with 5% skim dry milk in Tris-buffered saline (TBS; 150 mM NaCl, 100 mM Tris-HCl [pH 7.5], and 0.05% Nonidet P-40) for 1 h at 37°C. Antisera were diluted in TBS to the desired concentration and incubated with the nitrocellulose sheets for 1 h at 37°C. Unbound antibodies were removed by washing the sheets three times in TBS, which was followed by the reaction with the second antibody, an alkaline phosphatase-conjugated goat anti-rabbit immunoglobulin G (Dianova) diluted 1:7,000 in TBS, for 1 h at 37°C. After the sheets were rinsed with TBS, bound phosphatase-conjugated antibodies were detected by reacting with 70 μg of nitroblue tetrazolium chloride (Biomol) per ml and 35 μg of 5-bromo-4-chloro-3-indolylphosphate (Biomol) per ml in alkaline phosphatase buffer (100 mM NaCl, 50 mM $MgCl_2$, 100 mM Tris-HCl, pH 9.5). The reaction was stopped with 20 mM Tris-HCl (pH 8)–5 mM EDTA.

Surface proteolysis of *M. pneumoniae*. To detect surface-exposed regions of the P65 protein, mild surface proteolysis was performed with intact cells. *M. pneumoniae* cells were harvested as described above and suspended in PBS (2 mg of protein per ml), and a 2-ml sample was subjected to proteolysis. As control, a 400-μl sample of untreated cells was removed. To the remaining cell suspension 7 μg (2.3 U) of proteinase K (Fluka) was added. After 5, 10, or 15 min of incubation at room temperature the cleavage was terminated by mixing of 400-μl samples with 4 μl of 1 M EDTA. The cells were pelleted as described above and lysed in 300 μl of Laemmli sample buffer. The same procedure was performed using 150 μg α-chymotrypsin (Sigma) per ml with the exception that the reaction took place at 37°C and was stopped with 10 U of aprotinin per ml. For Western blot analysis, 10-μl samples per lane were loaded on SDS–12% polyacrylamide gels.

Immunoadsorption experiment. The method of Engleberg et al. (16) was applied to determine whether the anti-fusion protein (FP) F10-2D (P65) antiserum recognizes surface-exposed epitopes. The FP-specific antiserum was produced in rabbits as described previously (45). The region of P65 that correlates to the FP is indicated in Fig. 5. *M. pneumoniae* cells (50 mg [net weight]) were suspended in 1 ml of PBS containing 0.5 mM $MgCl_2$ and 0.15 mM $CaCl_2$ and supplemented with 10 μl of anti-FP F10-2D (P65) antiserum. After incubation overnight at 4°C with gentle shaking, the cells were washed three times in PBS. The bound antibodies were eluted by suspending the cells in 1 ml of 0.2 M NaCl–0.2 M glycine-HCl, pH 2.8, and incubating them for 30 min at room temperature. The cells were pelleted, and the supernatant was neutralized with 100 μl of 2 M Tris-HCl, pH 8.8, and tested for the presence of immunoreactive anti-P65 antibodies by immunoblot analysis. As a control, the test was also applied with antiserum against FP D2-5E (ATP-synthase α-chain) (45).

Immunofluorescence tests. *M. pneumoniae* M129 cells were grown on chamber slides (Nunc) for 2 days at 37°C. The glass-attached bacteria were washed three times in PBS and fixed with 2% paraformaldehyde in PBS for 30 min at room temperature. After a further wash step the cells were incubated with a solution of 1% bovine serum albumin in PBS for 30 min at 37°C. The anti-FP F10-2D (P65) serum was diluted 1:50 in PBS and incubated with the prepared cells (200 μl per chamber) for 1 h at 37°C. As negative controls, preimmune serum and antiserum against FP G7-3A (elongation factor G [EF-G]) were used in similiar dilutions. Antiserum against FP E7B 20 (P1 protein) (45) was used as a positive control. After the slides were washed three times with PBS, 100 μl of fluorescein (DTAF)-conjugated anti-rabbit immunoglobulin G (heavy and light chains) (Dianova) diluted 1:100 in PBS was added to each chamber and incubated for 1 h at 37°C. The slides were washed again two times in PBS and one time in double-distilled water, air dried, and examined with a Zeiss epifluorescence microscope.

Nested deletion clones and DNA sequence analysis. Plasmid pF10/5.1, a subclone of pcos MP F10 (56, 57), was used for creating nested deletion clones. The plasmid was linearized with endonucleases *Apa*I and *Xho*I and then subjected to an unidirectional controlled exonuclease digestion (23a) with an exonuclease III kit (Pharmacia). Sixteen deletion mutants were selected according to size after electrophoresis on a 1% agarose gel. The selected plasmids were purified by the rapid alkaline lysis method (48), phenol-chloroform extracted, ethanol precipitated, and resuspended in TE (10 mM Tris-HCl [pH 8], 0.1 mM EDTA). DNA sequencing was performed by the chain termination method (49) using *Taq* polymerase and fluorescently tagged primers or dideoxynucleotides in conjunction with an ABI 373A automated sequencer. Dye-labelled universal primer M13 (−21) (Applied Biosystems) was used for DNA sequencing of the deletion clones. The remaining gaps and the complementary DNA strand were sequenced by primer walking with custom-made oligonucleotides.

Cloning of the F10/5.1-analogous *Eco*RI fragment of *M. pneumoniae* FH. Genomic DNA of *M. pneumoniae* FH was fully digested with endonuclease *Eco*RI and ligated into plasmid vector pBC SK(+) (Stratagene). *E. coli* XL1-Blue cells were transformed, and colonies were transferred onto Biodyne B nylon membranes (Pall), pretreated with 10% SDS, denatured with 1.5 M NaCl–0.5 M NaOH, and neutralized with 0.5 M Tris-HCl, pH 8.0. After baking at 80°C for 1 h, the filters were preincubated at 37°C for 3 h in hybridization buffer (5× SSC [i.e., 750 mM NaCl, 75 mM sodium citrate, pH 7.2], 10× Denhardt's solution [i.e., 0.2% Ficoll, 0.2% polyvinylpyrrolidine, 0.2% bovine serum albumin], 0.1% SDS) supplemented with 50 μg of denatured herring sperm DNA per ml. Oligonucleotide F10/5.1-E (5′GCTCAAAGACAAGTTAGAT3′) served as a specific probe. It was originally used as a sequencing primer for the F10/5.1 *Eco*RI fragment of *M. pneumoniae* M129. After the 5′ end was labelled with ^{32}[γ-^{32}P]ATP by the method of Maxam and Gilbert (40), it was added to hybridization buffer (1.5×10^6 cpm/10 ml) and incubated with the filters overnight at 37°C. The filters were washed twice with 5× SSC–0.1% SDS at 37°C for 30 min and exposed to X-ray films (Kodak).

Plasmid pF10/5.1 (FH) was purified with a midicolumn of the Qiagen DNA purification kit (Qiagen). The FH P65 ORF ($orfp65_{FH}$) was analyzed by DNA sequencing one strand only, using the oligonucleotides that originally were generated for sequencing $ORFP65_{M129}$ by primer walking.

Computer-assisted analyses. Computer analyses were performed with the program package HUSAR (Heidelberg Unix Sequence Analysis Resources), release 3.0, at the German Cancer Research Center, Heidelberg, Germany. The program FASTA (36) was used for searching the SwissProt and PIR protein databases. Conserved peptide motifs were evaluated by the PROSITE program (1). Protein structure analyses were carried out with the programs PEPTIDESTRUCTURE, PEPPLOT, and PEPCOIL. DNA sequences were aligned with the GAP program, using the algorithm of Needleman and Wunsch (42).

Nucleotide sequence accession numbers. The nucleotide and deduced amino acid sequences for $orfp65_{M129}$ and $orfp65_{FH}$ have been submitted to the EMBL gene bank under accession numbers Z34977 and Z34978, respectively.

RESULTS

Detection of P65 in Triton X-100-insoluble subfractions. Protein P65 is enriched in the Triton X-100-insoluble fraction of *M. pneumoniae* M129. This fraction still shows a complex protein pattern on stained polyacrylamide gels (Fig. 1, lanes 1). Triton X-100-insoluble material was further fractionated with sequentially increasing concentrations of $MgCl_2$, KJ, and urea, respectively. Each subfraction was examined for the presence of P65 by immunoblot analysis with anti-FP F10-2D antiserum (anti-P65 antiserum).

Treatment of the Triton X-100-insoluble fraction with $MgCl_2$ resulted in partial release of P65 with 1, 2, and 3 M $MgCl_2$, leaving the major portion of P65 still associated within the insoluble fraction even after treatment with 4 M $MgCl_2$ (Fig. 1B, left part). All other proteins showed very poor solubility in $MgCl_2$ with the exception of an unknown 30-kDa protein that was enriched in the 3 M $MgCl_2$-soluble fraction (Fig. 1A, left part).

KJ showed a significantly higher efficiency in liberating proteins from the Triton X-100-insoluble fraction. The majority of P65 could be detected in the 1 M KJ-soluble fraction. The remaining part was totally released with 3 M KJ (Fig. 1B, central part), whereas most of the other proteins were released

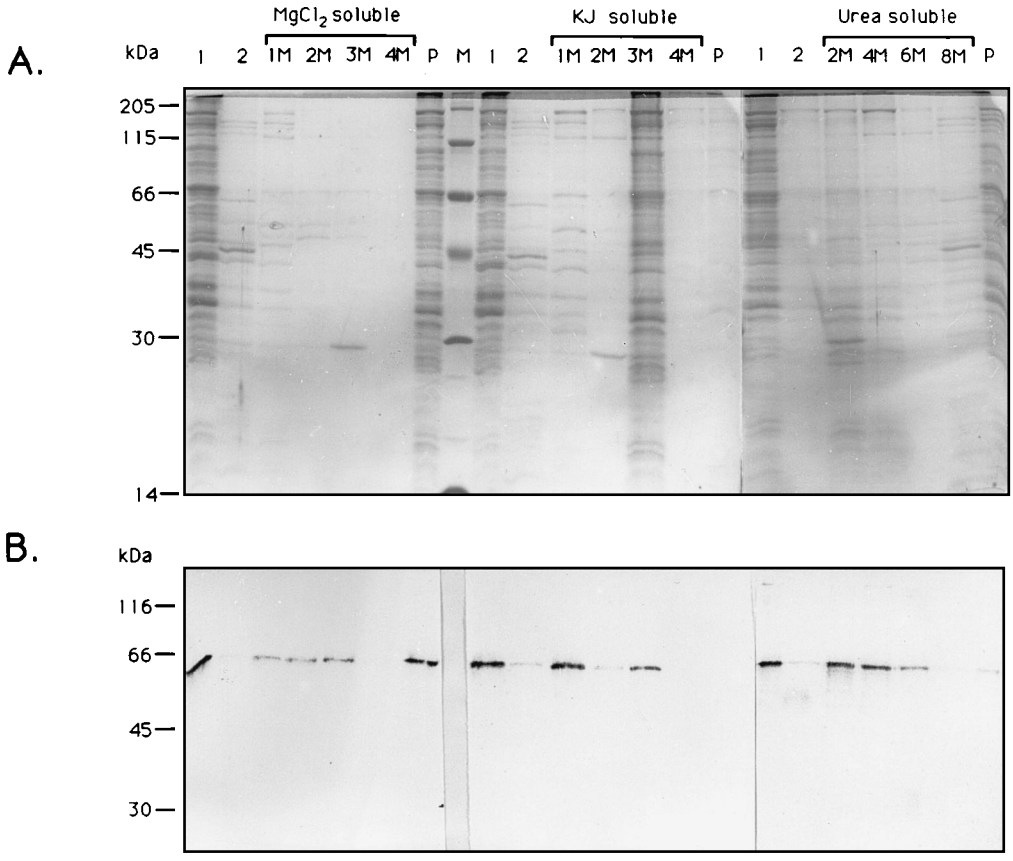

FIG. 1. (A) Silver-stained SDS–12% polyacrylamide gel of Triton shell proteins extracted with the indicated increasing concentrations of $MgCl_2$, KJ, and urea. The solubilized proteins were precipitated, and all the pellets were resuspended in equal volumes of sample buffer to reflect the real protein distribution. Lanes: 1, Triton X-100-insoluble fraction (Triton shell); 2, proteins washed from the Triton shell with 0.6 M KCl–1 mM EDTA; P, insoluble protein pellet after individual extraction steps; M, molecular mass standards (Sigma). (B) Immunoblot analysis with anti-FP F10-2D (P65) antiserum. The corresponding polyacrylamide gel was loaded as described for panel A.

from the insoluble material only after treatment with 3 M KJ. (Fig. 1A, central part).

Urea was more efficient in liberating proteins from the Triton X-100-insoluble fraction than $MgCl_2$ and less efficient than KJ: a significant amount of protein was still associated with the Triton X-100-insoluble fraction after treatment with 8 M urea (Fig. 1A, right part). P65 was enriched mainly in the 2 and 4 M urea-soluble fractions (Fig. 1B, right part). We also tested the distribution of HMW1 and HMW3, which are considered typical components of the Triton X-100-insoluble fraction under the same conditions. Both proteins were preferentially liberated from the Triton X-100-insoluble fraction by treatment with 6 M urea but were absolutely insoluble in 4 M $MgCl_2$ (data not shown). These results indicate that P65 is more weakly associated with the Triton X-100-insoluble fraction than are most proteins, including HMW1 and HMW3.

Proteolysis of surface proteins. To localize the P65 protein in the cell, we studied the probable surface exposure of P65 by surface proteolysis of intact cells using proteinase K and α-chymotrypsin. The cell lysates were analyzed with anti-P65 antiserum in Western blots. To ensure optimal protease concentrations, antiserum against P1 protein and EF-G served as controls. P1 is the major adhesin of *M. pneumoniae* (3, 25), and EF-G is a cytosolic protein. The control experiments showed that the proteinase K concentration used for the cleavage experiment is critical, since the range of protease concentration necessary for complete cleavage of P1 without affecting EF-G was very narrow (0.8 to 1.2 U/ml).

Immunoblot analysis with anti-FP F10-2D (P65) antiserum showed a very limited cleavage of P65 with both proteinase K and α-chymotrypsin (Fig. 2). Even after 15 min of incubation, less than 20% of P65 was partially cleaved and the remaining 80% of P65 was not affected at all. Protease treatment of cells pretreated with 0.1% Triton X-100 resulted in complete cleavage of P65.

Immunofluorescence experiments. *M. pneumoniae* cells grown on chamber slides were fixed with paraformaldehyde and used for immunofluorescence assays with anti-FP F10-2D (P65) antiserum. Preimmune serum and antiserum against EF-G served as negative controls, and anti-P1 antiserum served as a positive control.

The bacteria showed a positive immunofluorescence with the anti-P65 antiserum (Fig. 3A), although the reactivity was not as strong as with the anti-P1 antiserum (data not shown). Preimmune serum (Fig. 3B) and anti-EF-G antiserum gave negative results. These results indicate the presence of surface-exposed epitopes within the P65 protein.

Immunoadsorption assay. To evaluate the binding of anti-FP F10-2D (P65) antibodies to surface-exposed regions, we adsorbed antisera against P65 and EF-G with intact *M. pneumoniae* cells. The anti-P65 antibodies eluted from the cells showed positive reactivity in immunoblot analysis. Under the

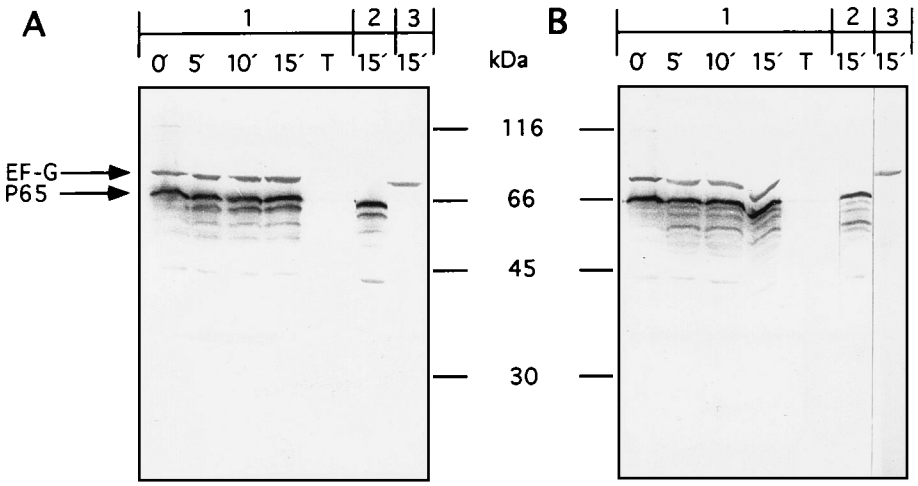

FIG. 2. Immunoblot analysis showing the partial time-dependent surface proteolysis of P65. Whole *M. pneumoniae* cells were treated with proteinase K (A) and α-chymotrypsin (B). The reactions were stopped after 5, 10, and 15 min as indicated, and lysates were loaded on an SDS–12% polyacrylamide gel. The immunoblots were analyzed with a mixture of anti-FP F10-2D (P65) and anti-FP G7-3A (EF-G) antiserum (lanes 1) and, separately, with anti-FP F10-2D antiserum (lanes 2) or anti-FP G7-3A antiserum (lanes 3). In *M. pneumoniae* cells pretreated with 0.1% Triton X-100 (lanes T) both P65 and EF-G are completely cleaved after 15 min.

same conditions anti-ATP-synthase α-chain antibodies could not be eluted from the cells (data not shown). Since ATP-synthase α-chain is located at the cytoplasmatically oriented side of the cell membrane, damaging of the cells during incubation in PBS can be excluded.

Detection of a variant P65 in *M. pneumoniae* FH. Differences in DNA and protein profiles were detected among clinical isolates of *M. pneumoniae* (47, 54, 55). On the basis of restriction fragment length polymorphism of the P1 gene *M. pneumoniae* isolates were classified in two distinct categories: group I, containing M129, and group II, containing the FH strain (11, 54). We looked for possible diversity of P65 in the two *M. pneumoniae* strains by screening whole-cell lysates on Western blots. P65 could be detected in both strains, but the FH strain expressed a larger variant of P65 with an estimated molecular mass of 68 kDa (Fig. 4).

DNA sequence analysis. orfp65 was localized on the 5.1-kbp *Eco*RI fragment of cosmid pcosMP F10 (a subclone of plasmid pF10/5.1) by Southern hybridization with radioactively labelled pF10-2D (expression vector isolated from a pcosMP F10 expression library and correlated to orfp65 [45]). A set of nested deletion clones was constructed from pF10/5.1 (see Materials and Methods), and the DNA was sequenced. The complete orfp65 could be identified by aligning the inserted DNA sequences of the expression plasmids pF10-2B and pF10-2D with the DNA sequence of pF10/5.1. The results indicated that the *M. pneumoniae* DNA of both expression vectors was in frame to one and the same ORF, consisting of 1,218 bases (Fig. 5). N-terminal sequencing of immunopurified P65 failed, probably because of a modified N-terminal amino acid. However, the proposed start codon is very likely because it is the only ATG

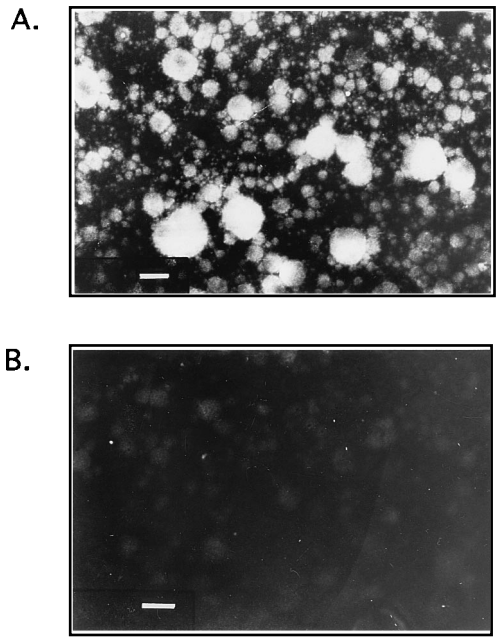

FIG. 3. Immunofluorescence of paraformaldehyde-fixed *M. pneumoniae* cells probed with anti-FP F10-2D (P65) antiserum (A) and anti-FP G7-3A (EF-G) (B) as a negative control. The positive fluorescence reaction indicates that P65 exhibits surface-exposed regions. Bars = 5 μm.

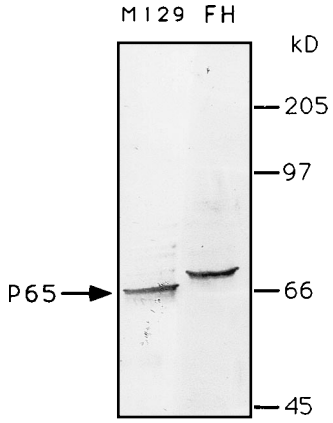

FIG. 4. Immunoblot analysis with cell lysates of *M. pneumoniae* M129 and FH probed with anti-FP F10-2D (P65) antiserum showing a size polymorphism of P65.

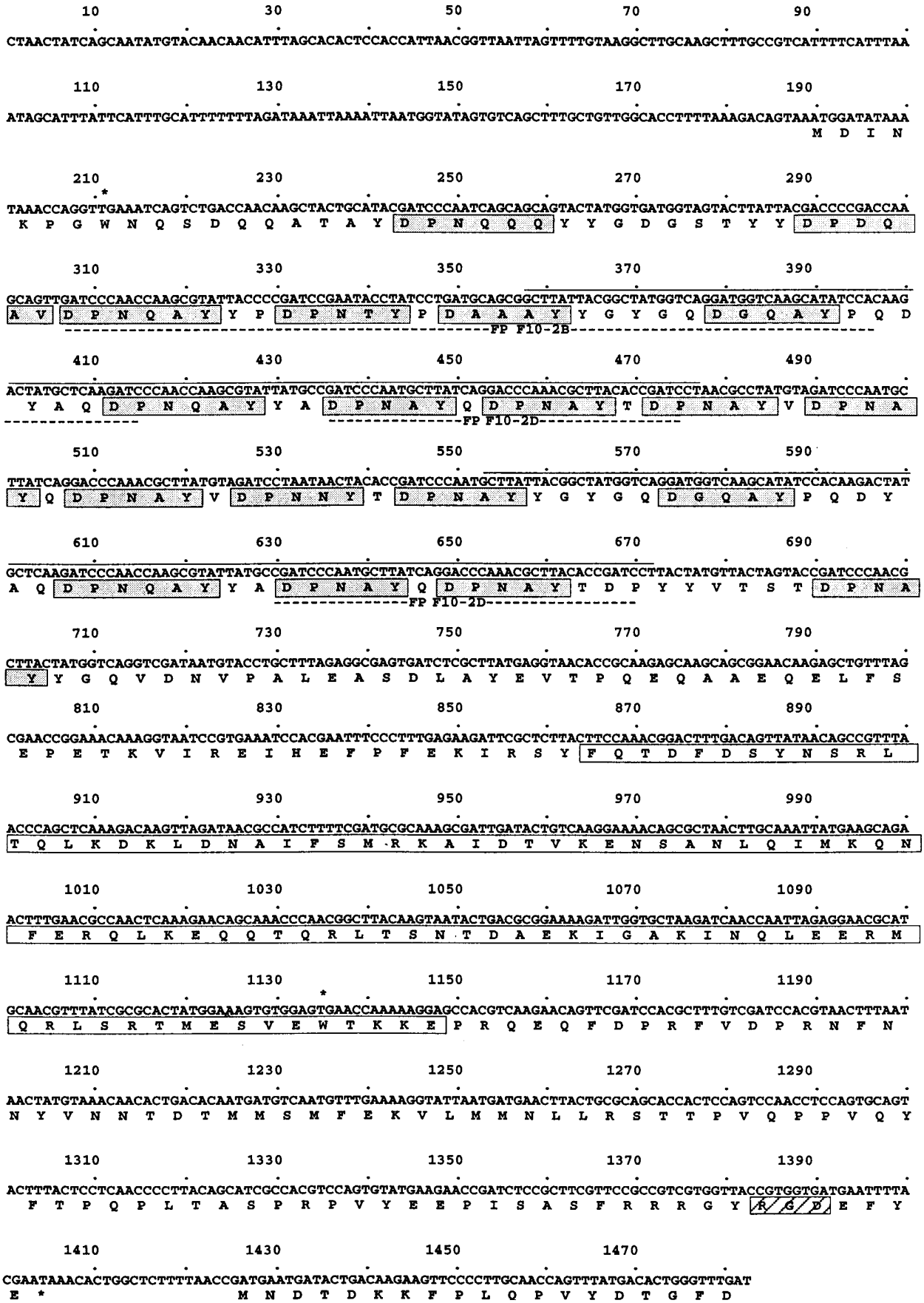
10 30 50 70 90
CTAACTATCAGCAATATGTACAACAACATTTAGCACACTCCACCATTAACGGTTAATTAGTTTTGTAAGGCTTGCAAGCTTTGCCGTCATTTTCATTTAA
110 130 150 170 190
ATAGCATTTATTCATTTGCATTTTTTTAGATAAATTAAAATTAATGGTATAGTGTCAGCTTTGCTGTTGGCACCTTTTAAAGACAGTAAATGGATATAAA
M D I N
210 230 250 270 290
TAAACCAGGTTGAAATCAGTCTGACCAACAAGCTACTGCATACGATCCCAATCAGCAGCAGTACTATGGTGATGGTAGTACTTATTACGACCCCGACCAA
K P G W N Q S D Q Q A T A Y D P N Q Q Q Y Y G D G S T Y Y D P D Q
310 330 350 370 390
GCAGTTGATCCCAACCAAGCGTATTACCCCGATCCGAATACCTATCCTGATGCAGCGGCTTATTACGGCTATGGTCAGGATGGTCAAGCATATCCACAAG
A V D P N Q A Y Y P D P N T Y P D A A A Y Y G Y G Q D G Q A Y P Q D
FP F10-2B
410 430 450 470 490
ACTATGCTCAAGATCCCAACCAAGCGTATTATGCCGATCCCAATGCTTATCAGGACCCAAACGCTTACACCGATCCTAACGCCTATGTAGATCCCAATGC
Y A Q D P N Q A Y Y A D P N A Y Q D P N A Y T D P N A Y V D P N A
FP F10-2D
510 530 550 570 590
TTATCAGGACCCAAACGCTTATGTAGATCCTAATAACTACACCGATCCCAATGCTTATTACGGCTATGGTCAGGATGGTCAAGCATATCCACAAGACTAT
Y Q D P N A Y V D P N N Y T D P N A Y Y G Y G Q D G Q A Y P Q D Y
610 630 650 670 690
GCTCAAGATCCCAACCAAGCGTATTATGCCGATCCCAATGCTTATCAGGACCCAAACGCTTACACCGATCCTTACTATGTTACTAGTACCGATCCCAACG
A Q D P N Q A Y Y A D P N A Y Q D P N A Y T D P Y Y V T S T D P N A
FP F10-2D
710 730 750 770 790
CTTACTATGGTCAGGTCGATAATGTACCTGCTTTAGAGGCGAGTGATCTCGCTTATGAGGTAACACCGCAAGAGCAAGCAGCGGAACAAGAGCTGTTTAG
Y Y G Q V D N V P A L E A S D L A Y E V T P Q E Q A A E Q E L F S
810 830 850 870 890
CGAACCGGAAACAAAGGTAATCCGTGAAATCCACGAATTTCCCTTTGAGAAGATTCGCTCTTACTTCCAAACGGACTTTGACAGTTATAACAGCCGTTTA
E P E T K V I R E I H E F P F E K I R S Y F Q T D F D S Y N S R L
910 930 950 970 990
ACCCAGCTCAAAGACAAGTTAGATAACGCCATCTTTTCGATGCGCAAAGCGATTGATACTGTCAAGGAAAACAGCGCTAACTTGCAAATTATGAAGCAGA
T Q L K D K L D N A I F S M R K A I D T V K E N S A N L Q I M K Q N
1010 1030 1050 1070 1090
ACTTTGAACGCCAACTCAAAGAACAGCAAACCCAACGGCTTACAAGTAATACTGACGCGGAAAAGATTGGTGCTAAGATCAACCAATTAGAGGAACGCAT
F E R Q L K E Q Q T Q R L T S N T D A E K I G A K I N Q L E E R M
1110 1130 1150 1170 1190
GCAACGTTTATCGCGCACTATGGAAAGTGTGGAGTGAACCAAAAAGGAGCCACGTCAAGAACAGTTCGATCCACGCTTTGTCGATCCACGTAACTTTAAT
Q R L S R T M E S V E W T K K E P R Q E Q F D P R F V D P R N F N
1210 1230 1250 1270 1290
AACTATGTAAACAACACTGACACAATGATGTCAATGTTTGAAAAGGTATTAATGATGAACTTACTGCGCAGCACCACTCCAGTCCAACCTCCAGTGCAGT
N Y V N N T D T M M S M F E K V L M M N L L R S T T P V Q P P V Q Y
1310 1330 1350 1370 1390
ACTTTACTCCTCAACCCCTTACAGCATCGCCACGTCCAGTGTATGAAGAACCGATCTCCGCTTCGTTCCGCCGTCGTGGTTACCGTGGTGATGAATTTTA
F T P Q P L T A S P R P V Y E E P I S A S F R R R G Y R/G/D E F Y
1410 1430 1450 1470
CGAATAAACACTGGCTCTTTTAACCGATGAATGATACTGACAAGAAGTTCCCCTTGCAACCAGTTTATGACACTGGGTTTGAT
E * M N D T D K K F P L Q P V Y D T G F D

FIG. 5. Nucleotide sequence of *M. pneumoniae* M129 DNA containing orfp65 with the single-letter code for the deduced P65 protein. The two 119-bp direct repeats within the proline-rich acidic domain are marked with solid lines. The sequences which could be correlated with the fusion proteins FP F10-2B and FP F10-2D are underlined with dashed lines. Because of the direct DNA repeat, the FP F10-2D appears two times. The DPN(Q)AY penta- or hexapeptides, which occur several times within the proline-rich acidic domain, are marked by shaded boxes. The RGD motif, which often plays a role in adhesion processes, was located near the C terminus (striped box). The two UGA opal termination codons which are used as Trp codons in *M. pneumoniae* (27) are marked by asterisks.

triplet between the FP F10-2B-related DNA region and the next in-frame stop codon upstream. No putative ORF could be detected upstream of the proposed start codon, but another ORF starts 19 nucleotides downstream of the orfp65 stop codon.

Computer-assisted analysis of P65. The predicted molecular weight of 47,034 calculated from the amino acid sequence deduced from ORFP65 does not agree with the molecular mass of 65 kDa estimated by SDS-PAGE. This phenomenon of abnormal gel migration was also described for the *M. pneumoniae* proteins HMW1 (13) and HMW3 (44) and for some cytoskeleton proteins of other organisms, e.g., articulin of *Euglena gracilis* (39). Like HMW1 and HMW3, the P65 protein has an unusually high Pro content (9.1%) and a low isoelectric point (pI = 4.09) caused by a high content of Asp and Glu residues (15.6%). It is noted in the literature that the classical SDS-PAGE method often overestimates molecular weights if the proline content is >10% in a given protein (20). Recently it could be demonstrated that a recombinant HMW1 protein expressed in *E. coli* showed an abnormal migration in SDS-PAGE similiar to that of the wild-type HMW1 (13), supporting the view that the amino acid composition, and not any other posttranslational modification, is causing this effect. On the basis of protein secondary-structure analysis according to the algorithms of Chou and Fasman (8) and Garnier et al. (21) (Fig. 6), P65 can be divided into three domains. The first domain (domain I), ranging from amino acid residues 1 to 180, is predicted to have mostly nonrepetitive conformations (turns or coils). Domain II (residues 180 to 320) is suggested to develop mainly α-helical structures. Moreover, the main part of this domain (residues 223 to 320) has a high probability for building coiled-coil structures, as could be predicted with the algorithm of Lupas et al. (37) (Fig. 6, bottom graph). Domain III, ranging from residues 320 to 405, showed a combination of α-helices, β-sheets, and turns.

The structure of the first domain might be influenced by the high content of proline (12%), which is responsible for the presence of the turns. The low pI of P65 (4.09) is caused mainly by domain I, on the basis of a high Asp content (13.5%) and the absence of positively charged amino acids (Fig. 6). Several peptide blocks with a similar composition bias were observed within the acidic proline-rich domain I. The pentapeptide DP NAY occurs nine times. Additionally, five modified repeats differing in one or two amino acids were observed. Furthermore, the hexapeptide DPNQAY was found in three complete and two modified repeats, and the pentapeptide PQDYA is repeated twice.

A part of the amino acid repeats is encoded by a 119-bp DNA segment that occurs twice as a perfect direct repeat (nucleotide positions 358 to 477 and 553 to 672; Fig. 5).

FP F10-2B and FP F10-2D, which were isolated by screening an *E. coli* expression library (45), both can be correlated to the proline-rich acidic domain of P65 (Fig. 5). Since FP F10-2D is very short, the epitope(s) for the monospecific anti-FP antibodies could be assigned to a very small region of 14 amino acids (DPNAYQDPNAYTDP) that includes two DPNAY pentapeptides. This region exists twice in the protein and in another copy with just one amino acid exchange (Val for Thr).

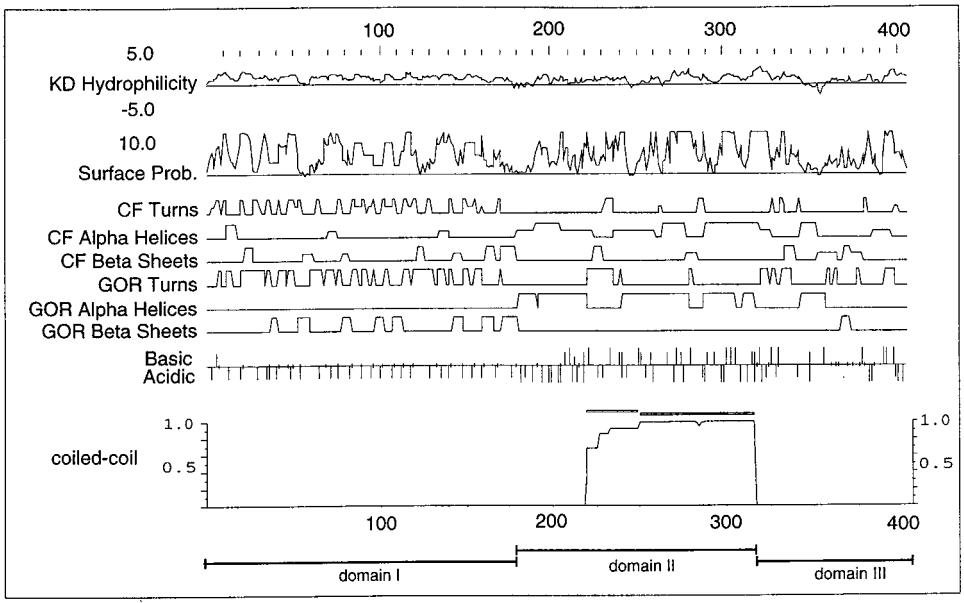

FIG. 6. Structural computer predictions based on the deduced amino acid sequence of P65. The scales at the top and the bottom indicate residue numbers. Analyses were performed by use of the PEPPLOT, PEPSTRUCTURE, and PEPCOIL programs of the HUSAR program package at the German Cancer Research Center (Heidelberg, Germany). KD hydrophilicity was calculated as described by Kyte and Doolittle (32). Surface probability was calculated as described by Emini et al. (15). Secondary structures were predicted by the methods of Chou and Fasman (CF) (8) and Garnier et al. (GOR) (21). The coiled-coil prediction is based on the algorithm of Lupas et al. (37).

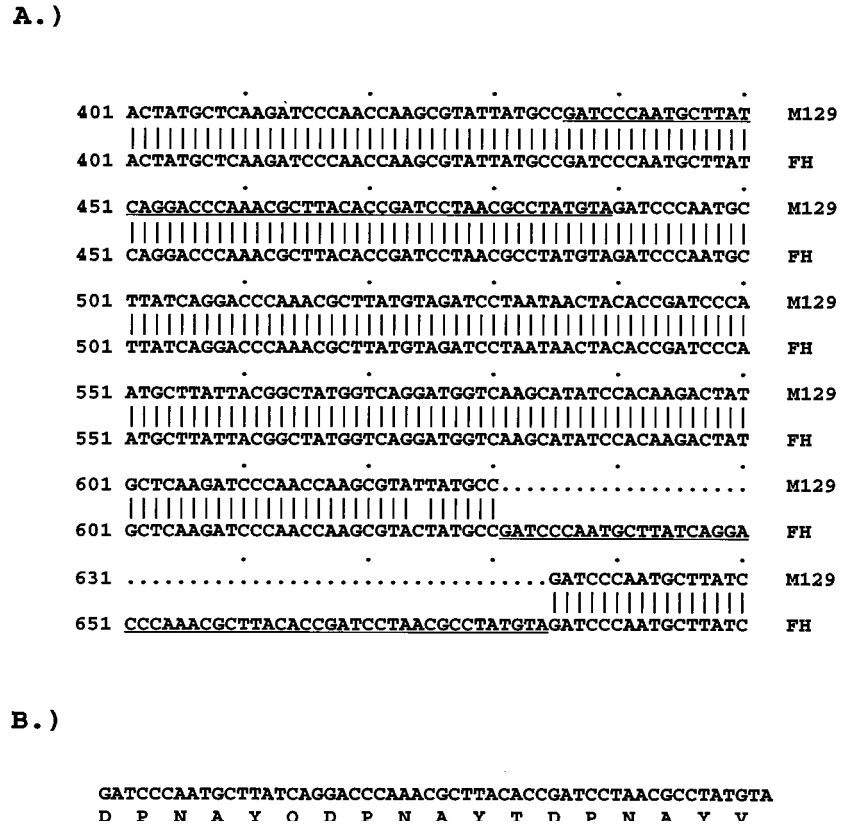

FIG. 7. (A) Part of a DNA sequence alignment of ORFP65 of *M. pneumoniae* M129 and FH, showing the intragenetic duplication of a 54-bp sequence. The two direct repeats are underlined. (B) Nucleotide sequence and deduced amino acid sequence of the duplicated region in the FH strain. The 54-bp region encodes three DPNAY pentapeptides, increasing the repeat number from 9 to 12.

A single DPNAY pentapeptide appears not to be sufficient for binding these antibodies, since the anti-FP F10-2D antibodies show no cross-reactivity with HMW3 containing two DPNAY repeats separated by 33 amino acids. We searched the PROSITE database (1) for conserved peptide motifs and found the motif Arg-Gly-Asp (RGD) in domain III near the C terminus, confined to residues 399 to 401. The RGD motif was described as an important binding motif for extracellular matrix proteins to integrins (14).

The hydrophilicity profile of Kyte and Doolittle (32) revealed high hydrophilicity for the whole protein except for a short region near the C terminus (Fig. 6, top graph). Although this is the only region that might represent a typical α-helical transmembrane domain, the sequence of hydrophobic amino acids seems to be too short for spanning the membrane. Since the protein does not contain a motif which is characteristic for lipoproteins, it is unlikely that P65 is anchored in the membrane by a fatty acid residue.

Comparison with protein databases did not reveal significant homologies with known proteins, apart from very limited homology with the circumsporozoite protein of *Plasmodium falciparum* (12), based on the similarity of the highly redundant tandemly ordered NANP tetrapeptides in the plasmodium protein to the DPN(Q)AY repeats of P65.

Analysis of the P65-analogous protein in the FH strain. The *Eco*RI fragment of *M. pneumoniae* FH, analogous to the M129 fragment of pF10/5.1, was cloned as described in Materials and Methods. Comparison of the two *Eco*RI fragments on agarose gels showed a slightly larger size for the FH-derived fragment, indicating a restriction fragment length polymorphism. To reveal the basis for the size polymorphism of the P65 proteins, the DNA sequences of orfp65 from both strains were aligned. In orfp65$_{FH}$ a duplication of a 54-bp region was observed at positions 435 to 489 according to the orfp65$_{M129}$ sequence: a perfect repeat was found in orfp65$_{FH}$, inserted at position 636 (Fig. 7A).

The deduced amino acid sequence of the 54-bp repeat showed that the DNA duplication was responsible for increasing the number of DNAPY pentapeptides from 9 to 12 repeats in P65$_{FH}$ (Fig. 7B). Besides the DNA duplication, three single-base-pair exchanges were observed on ORFP65$_{FH}$. An A-to-C transversion at nucleotide 207 and a T-to-C transition at nucleotide 624 occurred at the third position of the codon and therefore had no influence on amino acid composition. The third exchange, an A-to-G transition, was detected at nucleotide 202. This transition leads to an amino acid exchange from Lys to Glu at residue 5, replacing the sole basic amino acid in the acidic proline-rich domain by another acidic residue.

DISCUSSION

An insoluble protein network remains after treatment of whole *M. pneumoniae* cells with Triton X-100 (22, 41). This cell fraction still has a complex protein composition and also contains the cytadherence-associated proteins HMW1 to HMW5 (30, 31, 51–53). This report shows that P65, which is also a component of the Triton X-100-insoluble fraction, can be released more easily from this fraction under defined conditions

than most of the other insoluble proteins. These findings suggest that P65 is associated with the Triton X-100-insoluble protein network rather than being an integral part of it.

In our efforts to localize P65 in the *M. pneumoniae* cell, we applied different immunological approaches to detect P65 on the cell surface. Indeed, the results of various assays indicate that P65 may possess surface-exposed regions. Evidence for this assumption was achieved, first of all, by a positive immunofluorescence reaction with paraformaldehyde-fixed cells, using anti-FP F10-2D (P65) antiserum. Second, immunoadsorption experiments showed that the anti-FP antibodies recognize surface-exposed epitopes. Furthermore, mild treatment of whole cells with α-chymotrypsin and proteinase K resulted in cleavage of P65. However, only a small population of P65 molecules was affected by both proteases, and these P65 molecules were only partially cleaved. These results suggest that either (i) a small number of P65 molecules exhibit limited surface exposure and the remaining molecules are located inside the cell or (ii) all P65 molecules exhibit surface-exposed regions but are masked by an unknown component that hampered protease cleavage or/and are resistant to degradation because of a very compact and rigid protein conformation. Brewer et al. (6) reported that regularly repeating proline and charged residues imply an unusual conformation. They applied nuclear magnetic resonance spectroscopy for a protein segment of TonB containing Glu-Pro and Lys-Pro dipeptides separated by a linker region and revealed an extended rigid conformation that is resistant to denaturation and enzyme cleavage. False-positive results by damaging of cells during protease treatment or paraformaldehyde fixation, followed by entry of enzymes or antibodies into the cells, can be excluded as shown by the control experiments using antiserum against the cytosolic EF-G. If cells were pretreated with Triton X-100 prior to protease treatment, P65 was fully digested, indicating that the protein is protease sensitive outside its natural environment. However, we cannot rule out the possibility that the extraction procedure affected the protein conformation. Fixation of cells for immunofluorescence could also expose epitopes which under normal conditions are not accessible. On the other hand, the immunoadsorbance assay gave positive results with cells which were not pretreated. Thus, P65 (or at least a part of it) should be located on the cell surface as suggested by our immunological studies. However, P65 is highly hydrophilic, and no potential transmembrane domain can be detected. A parallel might be drawn to HMW3, which also has no putative membrane-spanning region, although biochemical and ultrastructural studies indicate that HMW3 is a membrane-spanning protein (44). This paradox might be explained by the existence of an atypical membrane-spanning structure. Evidence for this assumption comes from the finding that hydrophobic α-helices are not an essential prerequisite of integral membrane proteins (9). Proteins of the porin family which span the membrane by building a barrellike structure of β-sheets are an important example (43). Recently, it was shown that a coiled-coil peptide can be inserted into a phospholipid membrane (58). Since domain III of P65 is predicted to build a coiled-coil structure, based on a perfect amphipathic α-helix, it should be possible that this domain spans the membrane.

The two *M. pneumoniae* strains tested, the clinical isolate M129 and the laboratory high-passage strain FH, show size polymorphism of DNA restriction fragments (11, 47, 54). In this work, we could show a size polymorphism of P65 between M129 and FH, obviously caused by an intragenetic duplication of a 54-bp sequence in $orfp65_{FH}$. As a consequence, the FH strain expresses a protein of about 68 kDa estimated from SDS-PAGE, which contains three more DPNAY pentapeptides. Moreover, the orfp65s of both strains contain a perfect 123-bp direct repeat within the region that encodes the proline-rich acidic domain of P65 (Fig. 5). In general, perfect DNA repeats are prone to be eliminated or reshuffled by recombination. The stability of those intragenetic duplications in this very small genome indicates that the encoded DPN(Q)AY repeats may have an important function within P65, for example, the binding to a basic counterpart of other proteins through ionic interactions. Many eucaryotic membrane skeleton proteins, including spectrin, are characterized by internal repeats which function in binding of accessory proteins and dimerization (5).

In conclusion, even if the amino acid sequence of the P65 protein does not show significant homology to eucaryotic structural proteins of the cytoskeleton, there might be structural features in common with eucaryotic structural proteins which could be responsible for associating the P65 protein with the Triton X-100-insoluble fraction.

ACKNOWLEDGMENTS

We thank Margrit Ellis and Rainer Frank for synthesis of the oligonucleotides and Christine Clayton for critical reading of the manuscript.

This work was supported by a grant from the Bundesminister für Forschung und Technologie (BCT 0381-6), the Deutsche Forschungsgemeinschaft (He 780/5-1), and a scholarship from the University of Heidelberg to T.P.

REFERENCES

1. **Bairoch, A.** 1992. PROSITE: a dictionary of sites and patterns in proteins. Nucleic Acids Res. **20:**2013–2018.
2. **Barile, M. F., D. K. F. Chandler, H. Yoshida, M. W. Grabowski, R. Harasawa, and S. Razin.** 1988. Parameters of *Mycoplasma pneumoniae* infection in Syrian hamsters. Infect. Immun. **56:**2443–2449.
3. **Baseman, J. B., R. M. Cole, D. C. Krause, and D. K. Leith.** 1982. Molecular basis for cytadsorption of *Mycoplasma pneumoniae*. J. Bacteriol. **151:**1514–1522.
4. **Baseman, J. B., P. J. Morrison, D. Drouillard, S. B. Puleo, V. V. Tryon, and S. C. Holt.** 1987. Identification of a 32-kilodalton protein of *Mycoplasma pneumoniae* associated with hemadsorption. Isr. J. Med. Sci. **23:**474–479.
5. **Bennett, V.** 1990. Spectrin-based membrane skeleton: a multipotential adaptor between plasma membrane and cytoplasm. Physiol. Rev. **70:**1029–1060.
6. **Brewer, S., M. Tolley, I. P. Trayer, G. C. Barr, C. J. Dorman, K. Hannavy, C. F. Higgins, J. S. Evans, B. A. Levine, and M. R. Wormald.** 1990. Structure and function of X-Pro dipeptide repeats in the TonB proteins of *Salmonella typhimurium* and *Escherichia coli*. J. Mol. Biol. **216:**883–895.
7. **Bullock, W. O., J. M. Fernandez, and J. M. Short.** 1987. XL1-Blue: a high efficiency plasmid transformation recA *Escherichia coli* strain with beta-galactosidase selection. BioTechniques **5:**376.
8. **Chou, P. Y., and G. D. Fasman.** 1978. Empirical predictions of protein conformation. Annu. Rev. Biochem. **47:**251–276.
9. **Cowan, S. W., and J. P. Rosenbusch.** 1994. Folding pattern diversity of integral membrane proteins. Science **264:**914–916.
10. **Dallo, S. F., A. Chavoya, and J. B. Baseman.** 1990. Characterization of the gene for a 30-kilodalton adhesin-related protein of *Mycoplasma pneumoniae*. Infect. Immun. **58:**4163–4165.
11. **Dallo, S. F., J. R. Horton, C. J. Su, and J. B. Baseman.** 1990. Restriction fragment length polymorphism in the cytadhesin P1 gene of human clinical isolates of *Mycoplasma pneumoniae*. Infect. Immun. **58:**2017–2020.
12. **Dame, J. B., J. L. Williams, T. F. McCutchan, J. L. Weber, R. A. Wirtz, W. T. Hockmeyer, W. L. Maloy, J. D. Haynes, I. Schneider, D. Roberts, G. S. Sanders, E. P. Reddy, C. L. Diggs, and L. H. Miller.** 1984. Structure of the gene encoding the immunodominant surface antigen on the sporozoite of the human malaria parasite *Plasmodium falciparum*. Science **225:**593–599.
13. **Dirksen, L. B., T. Proft, H. Hilbert, H. Plagens, R. Herrmann, and D. C. Krause.** Unpublished data.
14. **D'Souza, S. E., M. H. Ginsberg, and E. F. Plow.** 1991. Arginyl-glycyl-aspartic acid (RGD): a cell adhesion motif. Trends Biochem. Sci. **16:**246–250.
15. **Emini, E. A., J. V. Hughes, D. S. Perlow, and J. Boger.** 1985. Induction of hepatitis A virus-neutralizing antibody by a virus-specific synthetic peptide. J. Virol. **55:**836–839.
16. **Engleberg, N. C., E. Pearlman, and B. I. Eisenstein.** 1984. *Legionella pneumophila* surface antigens cloned and expressed in *Escherichia coli* are trans-

located to the host cell surface and interact with specific anti-*Legionella* antibodies. J. Bacteriol. **160:**199–203.
17. **Feldner, J., U. Göbel, and W. Bredt.** 1982. *Mycoplasma pneumoniae* adhesin localized to tip structure by monoclonal antibody. Nature (London) **298:**765–767.
18. **Foy, H. M., G. E. Kenny, M. K. Cooney, and I. D. Allan.** 1979. Long term epidemiology of infections with *Mycoplasma pneumoniae*. J. Infect. Dis. **139:**681–687.
19. **Francoso, G., P. C. Hu, G. A. Meloni, and M. F. Barile.** 1994. Immunoblot analyses of chimpanzee sera after infection and after immunization and challenge with *Mycoplasma pneumoniae*. Infect. Immun. **62:**1008–1014.
20. **Furthmayer, H., and R. Timpl.** 1971. Characterization of collagen peptides by sodium dodecylsulfate-polyacrylamide electrophoresis. Anal. Biochem. **41:**510–516.
21. **Garnier, J., D. J. Osguthorpe, and B. Robson.** 1978. Analysis of the accuracy and implications of simple methods for predicting the secondary structure of globular proteins. J. Mol. Biol. **120:**97–120.
22. **Goebel, U., V. Speth, and W. Bredt.** 1981. Filamentous structures in adherent *Mycoplasma pneumoniae* cells treated with nonionic detergents. J. Cell Biol. **91:**537–543.
23. **Hayflick, L.** 1965. Tissue cultures and mycoplasmas. Tex. Rep. Biol. Med. **23:**285–303.
23a. **Henikoff, S.** 1987. Unidirectional digestion with exonuclease III in DNA sequence analysis. Methods Enzymol. **155:**156–165.
24. **Hixon, W. G., and D. G. Searcy.** 1993. Cytoskeleton in the archaebacterium *Thermoplasma acidophilum*? Viscosity increase in soluble extracts. BioSystems **29:**151–160.
25. **Hu, P. C., R. M. Cole, Y. S. Huang, J. A. Graham, D. E. Gardner, A. M. Collier, and W. J. Clyde.** 1982. *Mycoplasma pneumoniae* infection: role of a surface protein in the attachment organelle. Science **216:**313–315.
26. **Hu, P. C., A. M. Collier, and J. B. Baseman.** 1977. Surface parasitism by *Mycoplasma pneumoniae* of respiratory epithelium. J. Exp. Med. **145:**1328–1343.
27. **Inamine, J. M., K. C. Ho, S. Loechel, and P. C. Hu.** 1990. Evidence that UGA is read as a tryptophan codon rather than as a stop codon by *Mycoplasma pneumoniae*, *Mycoplasma genitalium*, and *Mycoplasma gallisepticum*. J. Bacteriol. **172:**504–506.
28. **Inamine, J. M., S. Loechel, and P. C. Hu.** 1989. Analysis of the nucleotide sequence of the P1 operon of Mycoplasma pneumoniae. Gene **73:**175–183.
29. **Kahane, I., S. Tucker, D. K. Leith, P. J. Morrison, and J. B. Baseman.** 1985. Detection of the major adhesin P1 in Triton shells of virulent *Mycoplasma pneumoniae*. Infect. Immun. **50:**944–946.
30. **Krause, D. C., D. K. Leith, and J. B. Baseman.** 1983. Reacquisition of specific proteins confers virulence in *Mycoplasma pneumoniae*. Infect. Immun. **39:**830–836.
31. **Krause, D. C., D. K. Leith, R. M. Wilson, and J. B. Baseman.** 1982. Identification of *Mycoplasma pneumoniae* proteins associated with hemadsorption and virulence. Infect. Immun. **35:**809–817.
32. **Kyte, J., and R. F. Doolittle.** 1982. A simple method for displaying the hydropathic character of a protein. J. Mol. Biol. **157:**105–132.
33. **Laemmli, U. K.** 1970. Cleavage of structural proteins during the assembly of the head of bacteriophage T4. Nature (London) **227:**680–685.
34. **Layh-Schmitt, G., and R. Herrmann.** 1992. Localization and biochemical characterization of the ORF6 gene product of the *Mycoplasma pneumoniae* P1 operon. Infect. Immun. **60:**2906–2913.
35. **Layh-Schmitt, G., and R. Herrmann.** 1994. Spatial arrangement of gene products of the P1 operon in the membrane of *Mycoplasma pneumoniae*. Infect. Immun. **62:**974–979.
36. **Lipman, D. J., and W. R. Pearson.** 1985. Rapid and sensitive protein similarity searches. Science **227:**1435–1441.
37. **Lupas, A., M. van Dyke, and J. Stock.** 1991. Predicting coiled coils from protein sequences. Science **252:**1162–1164.
38. **Maniloff, J.** 1981. Cytoskeleton elements in mycoplasmas and other procaryotes. BioSystems **14:**305–312.
39. **Marrs, J. A., and G. B. Bouck.** 1992. The two major membrane skeleton proteins (articulins) of *Euglena gracilis* define a novel class of cytoskeleton proteins. J. Cell Biol. **118:**1465–1475.
40. **Maxam, A. M., and W. Gilbert.** 1980. Sequencing end-labeled DNA with base-specific chemical cleavages. Methods Enzymol. **65:**499–560.
41. **Meng, K. E., and R. M. Pfister.** 1980. Intracellular structures of *Mycoplasma pneumoniae* revealed after membrane removal. J. Bacteriol. **144:**390–399.
42. **Needleman, S. B., and C. D. Wunsch.** 1970. A general method applicable to the search for similarities in the amino acid sequences of two proteins. J. Mol. Biol. **48:**443–453.
43. **Nikaido, H.** 1992. Porins and specific channels of bacterial outer membranes. Mol. Microbiol. **6:**435–442.
44. **Ogle, K. F., K. K. Lee, and D. C. Krause.** 1992. Nucleotide sequence analysis reveals novel features of the phase-variable cytadherence accessory protein HMW3 of *Mycoplasma pneumoniae*. Infect. Immun. **60:**1633–1641.
45. **Proft, T., and R. Herrmann.** 1994. Identification and characterization of hitherto unknown *Mycoplasma pneumoniae* proteins. Mol. Microbiol. **13:** 337–348.
46. **Razin, S., and E. Jacobs.** 1992. Mycoplasma adhesion. J. Gen. Microbiol. **138:**407–422.
47. **Ruland, K., R. Wenzel, and R. Herrmann.** 1990. Analysis of three different repeated DNA elements present in the P1 operon of *Mycoplasma pneumoniae*: size, number and distribution on the genome. Nucleic Acids Res. **18:**6311–6317.
48. **Sambrook, J., E. F. Fritsch, and T. Maniatis.** 1989. Molecular cloning: a laboratory manual, 2nd ed. Cold Spring Harbor Laboratory, Cold Spring Harbor, N.Y.
49. **Sanger, F., S. Nicklen, and A. R. Coulson.** 1977. DNA sequencing with chain-terminating inhibitors. Proc. Natl. Acad. Sci. USA **74:**5463–5467.
50. **Sperker, B., P.-C. Hu, and R. Herrmann.** 1991. Identification of gene products of the P1 operon of *Mycoplasma pneumoniae*. Mol. Microbiol. **5:**299–306.
51. **Stevens, M. K., and D. C. Krause.** 1990. Disulfide-linked protein associated with *Mycoplasma pneumoniae* cytadherence phase variation. Infect. Immun. **58:**3430–3433.
52. **Stevens, M. K., and D. C. Krause.** 1991. Localization of the *Mycoplasma pneumoniae* cytadherence-accessory proteins HMW1 and HMW4 in the cytoskeletonlike Triton shell. J. Bacteriol. **173:**1041–1050.
53. **Stevens, M. K., and D. C. Krause.** 1992. *Mycoplasma pneumoniae* cytadherence phase-variable protein HMW3 is a component of the attachment organelle. J. Bacteriol. **174:**4265–4274.
54. **Su, C. J., S. F. Dallo, H. Alderman, and J. B. Baseman.** 1991. Distinctions in DNA and protein profiles among clinical isolates of *Mycoplasma pneumoniae*. J. Gen. Microbiol. **137:**2727–2732.
55. **Vu, A. C., H. M. Foy, F. D. Cartwright, and G. E. Kenny.** 1987. The principal protein antigens of isolates of *Mycoplasma pneumoniae* as measured by levels of immunoglobulin G in human serum are stable in strains collected over a 10-year period. Infect. Immun. **55:**1830–1836.
56. **Wenzel, R., and R. Herrmann.** 1989. Cloning of the complete *Mycoplasma pneumoniae* genome. Nucleic Acids Res. **17:**7029–7043.
57. **Wenzel, R., E. Pirkl, and R. Herrmann.** 1992. Construction of an *Eco*RI restriction map of *Mycoplasma pneumoniae* and localization of selected genes. J. Bacteriol. **174:**7289–7296.
58. **Yu, Y., G. D. S. King, and Y. K. Shin.** 1994. Insertion of a coiled-coil peptide from influenza virus hemagglutinin into membranes. Science **266:**274–275.